

Indistinguishable single photons generated by a quantum dot under resonant excitation observable without postselection

Léonard Monniello,^{1,2} Antoine Reigue,^{1,2} Richard Hosten,^{1,2} Aristide Lemaitre,³ Anthony Martinez,³ Roger Grousson,^{1,2} and Valia Voliotis^{1,2,*}

¹UPMC Univ Paris 06, UMR 7588, Institut des NanoSciences de Paris, 4 Place Jussieu, F-75005 Paris, France

²CNRS, UMR 7588, Institut des NanoSciences de Paris, 4 Place Jussieu, F-75005 Paris, France

³CNRS, UPR 20, Laboratoire de Photonique et Nanostructures, Route de Nozay, F-91460 Marcoussis, France

(Received 31 March 2014; revised manuscript received 20 June 2014; published 21 July 2014)

We report on two-photon interference of highly indistinguishable single photons emitted by a quantum dot. Strictly resonant excitation with picosecond laser pulses has been used to prepare coherent states with a significantly increased coherence time ($T_2 \sim 1$ ns) and reduced lifetime ($T_1 \sim 650$ ps), as compared to a nonresonant excitation scheme. Indistinguishable photons, with visibilities greater than 70%, have been observed by measuring the Hong-Ou-Mandel dip without postselection of the interfering photons. Near-unity indistinguishable photons should be achievable by preventing fluctuations in the electrostatic environment in the vicinity of the dots, considered as an important source of decoherence.

DOI: [10.1103/PhysRevB.90.041303](https://doi.org/10.1103/PhysRevB.90.041303)

PACS number(s): 78.67.Hc, 71.35.-y, 78.47.D-, 78.55.Cr

Solid-state single-photon emitters have demonstrated, over the past decade, a high potential for novel applications in the fields of nanophotonics [1] and quantum information technology [2]. The requirements for efficient on-demand generation of single photons have been partially fulfilled by using quantum dots (QDs), which have a high internal quantum efficiency, embedded in microcavities or photonic crystals for a high luminescence extraction efficiency into a specific single mode [3]. Furthermore, quantum computing schemes with linear optics and quantum teleportation [4] require indistinguishable photons, a fundamental property which can be tested by two-photon interference on a beam splitter (BS) in a Hong-Ou-Mandel (HOM) experiment [5]. Such two-photon interference experiments have been realized in the past few years using single photons emitted by a QD. Nevertheless, polarization postselection or spectral filtering prevents efficient generation of indistinguishable photons, and incoherent excitation is a limitation in obtaining highly coherent photons [6–8]. Ideally, the photons must be Fourier-transform limited, so the coherence time is truly limited by the radiative lifetime. However, for a solid-state emitter such as a QD, this is at present difficult to achieve. QDs strongly interact with their environment mainly through phonons and trapped charges, leading to dephasing processes [9]. A necessary condition to preserve the coherence is the resonant excitation of the QD two-level system [10], resulting in an increased coherence time T_2 and a reduced spontaneous emission rate T_1 without the need for a cavity [11,12]. Moreover, pulsed excitation rather than continuous-wave laser excitation must be used in order to generate single photons in a deterministic way [13,14]. An on-demand near-unity indistinguishable photon source will open the way for the efficient generation of entangled photon pairs from either a single QD or from several remote emitters [15].

In this Rapid Communication, we report on highly indistinguishable nonpostselected single photons emitted by

a single InAs/GaAs QD under resonant picosecond (ps) pulsed excitation. The QD two-level system is addressed with π pulses corresponding to a maximum population of the excited level, a neutral exciton in our case. Independent measurements of the lifetime T_1 and coherence time T_2 show a degree of indistinguishability $T_2/2T_1 \sim 0.7$. Second-order correlation measurements of the photoluminescence show an antibunching of the order of $g^2(0) = 0.07$, with a very low background and without any laser filtering. Two-photon interference on a beam splitter (BS) of two single-photon wave packets without postselection shows a maximum visibility of 0.73, in very good agreement with the direct measurements of T_1 and T_2 . Varying the delay between the arrival time of the two photons on the BS allows the HOM dip to be observed. The measurements agree very well with the theoretical dependence of the second-order correlation function on the delay time [16] without any adjustable parameters.

InAs/GaAs self-assembled QDs were grown by molecular beam epitaxy (MBE) on a planar (001) GaAs substrate and embedded in a planar microcavity made of unbalanced AlGaAs/GaAs Bragg mirrors, with 24 pairs below and 12 pairs above the QDs [Fig. 1(a)]. These Bragg mirrors enhance the luminescence collection efficiency by a factor of 20–50 times. The quality factor of the structure is low, around 500, so there is no significant Purcell effect. Finally, to create single-mode one-dimensional waveguides, ridges ranging from 0.8 to 1.2 μm wide were etched approximately 1.5 μm deep by inductively coupled plasma etching. Passivation of the surface has further improved the quality of the heterointerfaces, leading to an important suppression of the scattered laser and allowing the realization of the present experiments. The QDs are excited along the waveguide by ps pulses from a tunable mode-locked Ti:sapphire laser whose polarization is set along the y axis [Fig. 1(a)]. Then, on resonance, a single eigenstate of the fine structure split exciton state is addressed. This geometry is effective in avoiding any collection of the laser light and enhances the light-matter interaction, since the laser is confined in the guided mode and the QD luminescence is collected from the ridge top surface by a confocal microscope [Figs. 1(a) and 1(b)]. The spectra are almost background free,

*voliotis@insp.jussieu.fr

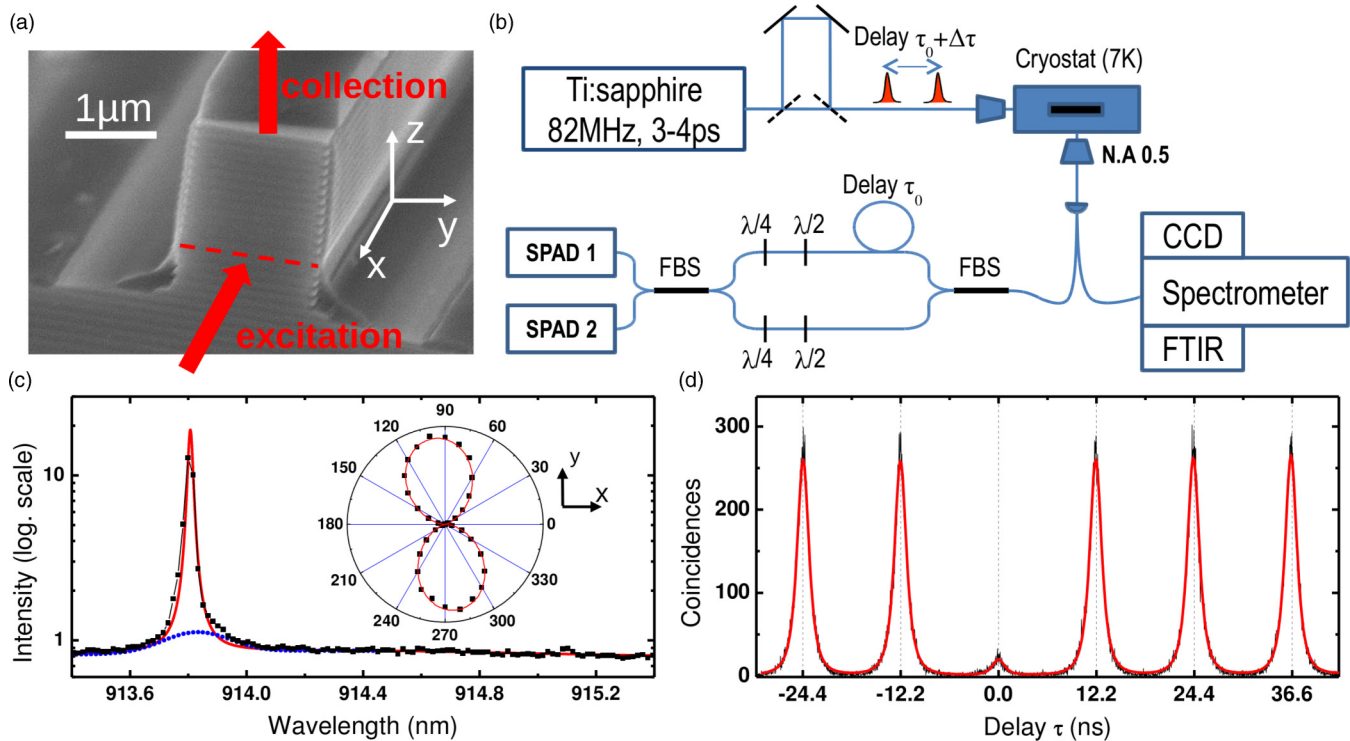


FIG. 1. (Color online) (a) Scanning electron microscope (SEM) image of one ridge. One can see the Bragg mirrors above and under the QD layer, whose position is marked by a red dashed line. Red arrows show the excitation and the collection paths. (b) Schematic drawing of the experimental setup. A pulsed ps Ti:sapphire laser comes through a first delay line, resulting in two pulses separated by $\tau_0 \pm \Delta\tau$ with $\tau_0 = 3$ ns every 12.2 ns. The luminescence is collected by a large numerical aperture (NA) microscope objective, coupled into an optical fiber and sent either into a spectrometer, or a fibered Mach-Zehnder interferometer with two fibered BSs with a fixed τ_0 delay for photon correlation studies. A fibered polarization setup equivalent to one $\lambda/2$ and $\lambda/4$ plates compensates the birefringence induced by the optical fibers. (c) Resonant spectrum in a semilogarithmic scale of the studied QD at 7 K: Experimental data (black dots) are fitted with a Lorentzian line (red line) and a wide Gaussian (blue dotted line) corresponding to the scattered laser. The inset shows the polar diagram of the QD resonant emission. (d) Second-order correlation function $g^2(\tau)$. At zero delay $g^2(0) = 0.07$ is obtained by normalizing the central peak integrated intensity by the average area of the five adjacent peaks. The fitting function for each peak is an exponential decay with the exciton radiative lifetime.

and strictly resonant experiments can be performed without any need for further polarization filtering [Fig. 1(c)]. The polar diagram in the inset of Fig. 1(c) shows that the emission of the QD investigated is linearly polarized, characteristic of a neutral exciton [17]. The luminescence is coupled into a single-mode optical fiber that can be connected to different setups either for spectroscopy, or first- and second-order correlation measurements [Fig. 1(b)]. Our setup enables the detection of 250 000 counts per second on a single-photon avalanche detector (SPAD).

It is worth noting that resonant excitation is not systematically observed for all the probed QDs. Indeed, it has been reported that resonant excitation can be suppressed due to the presence of trapped charges in the vicinity of the QDs [18]. In that case, adding a very low power He-Ne laser helps to recover the resonant luminescence. In the following, all the experiments are performed with π pulses on resonance with the neutral exciton and an additional He-Ne laser (a few pW) in most of the cases.

As expected, the emission statistics of a QD under resonant excitation corresponds to a single-photon source. Second-order correlation measurements $g^{(2)}(\tau)$ have been performed [Fig. 1(d)] with 120 000 counts/s on each SPAD after 1 h acquisition time. τ is the relative delay time between a photon

detection on SPAD1 and one photon detection on SPAD2. A clear antibunching is shown with a very low multiphoton probability of $g^2(0) = 0.07$ in Fig. 1(d). Neither polarization filtering nor spectral selection has been used to suppress the scattered laser. The remaining background in the second-order correlation measurement corresponds exactly to the scattered laser intensity observed in Fig. 1(c) (blue line).

The radiative lifetime T_1 has been measured to be $T_1^{\text{NR}} = 850$ ps under nonresonant excitation and $T_1^{\text{R}} = 670$ ps for on-resonance excitation. Normalized data are shown in a semilogarithmic plot in Fig. 2(a), where the time delay between the two curves is due to the radiative cascade that occurs while exciting nonresonantly at high energy [19]. The difference in the radiative lifetime under different excitation conditions has been previously experimentally observed [12] and can be explained by the strong coupling regime achieved between the QD and the field under resonant excitation [11]. We believe that the resonant coupling modifies the optical density of states, hence inducing a modification of the radiative decay rate similar to a Purcell effect [20,21].

The coherence time T_2 corresponding to the width of the luminescence line has been measured by Fourier transform spectroscopy using a Michelson interferometer with a variable path length δt , labeled FTIR in Fig. 1(b). The contrast of

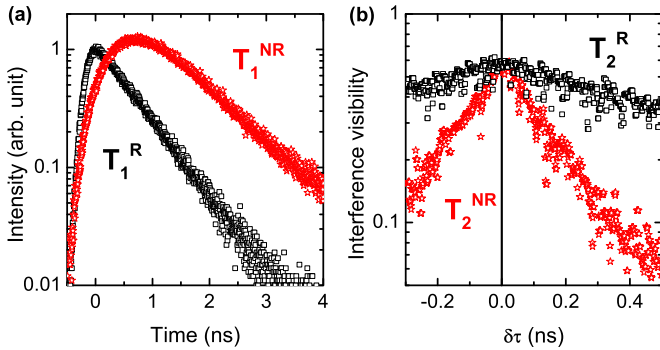


FIG. 2. (Color online) (a) Lifetime measurements (semilog scale) for resonant (black squares) and nonresonant (red stars) excitation. The temporal decays give $T_1^R = 670$ ps and $T_1^{NR} = 850$ ps. (b) Fourier transform spectra (semilog scale) for resonant (black squares) and nonresonant (red stars) excitation, yielding the coherence times $T_2^R = 950$ ps and $T_2^{NR} = 200$ ps.

the interference fringes as a function of the delay [Fig. 2(b)] is adjusted by a Voigt profile with 10% of inhomogeneous contribution. It gives typical values of $T_2^R = 900$ ps and $T_2^{NR} = 200$ ps for resonant and nonresonant excitation, respectively. This is due to the fact that for nonresonant excitation, electron-hole pairs are photocreated at high energy in the wetting layer and coherence is lost after relaxation into the dot. On the contrary, resonant excitation addresses directly the excited state of the QD and coherence is preserved.

Variations of the resonant coherence time between 850 and 950 ps were observed from day to day on the same dot, as well as variations of the inhomogeneous contribution of the Voigt profile. This effect has been attributed to the fluctuating electrostatic environment [8,22]. Indeed, the daily thermal cycling of the sample can lead to trapping of charges on defects close to the QDs, resulting in a different electrostatic environment seen by the dot. Spectral diffusion can occur and an inhomogeneous broadening of the emission line is observed in this case [23]. A similar behavior has been observed for the radiative lifetime which varies slightly from 650 to 700 ps. This effect can also be explained by the local modification of the electrostatic potential that alters the overlap of the hole and electron wave functions inside the dot, thus modifying the transition probability. The fluctuating electrostatic environment has also been indirectly observed

through a reduction of the resonant luminescence intensity. In that case, the presence of a residual charge in the QD, or tunneling of nearby trapped charges into the QD, can modify the first excited state from a neutral to a charged exciton, therefore suppressing the resonance with the excitation laser as reported in Ref. [18]. To circumvent this problem we used a very low power (few pW) He-Ne laser and the neutral exciton resonant luminescence intensity was increased tenfold, from 25 000 to 250 000 counts/s on the SPAD. The effect of the additional He-Ne laser is to generate carriers that neutralize the structural defects surrounding the QD on a long time scale, allowing one to recover the resonant emission by switching back the QD to a neutral state. Laser scattering and luminescence due to the He-Ne laser solely has been estimated to be less than 100 counts/s, comparable to the detector's dark counts.

In a two-photon interference experiment, two indistinguishable photons arriving at the same time on a 50/50 BS coalesce and emerge along the same output port of the BS [24]. Then, no simultaneous detection occurs on the two output detectors. The setup for the realization of the HOM experiment is shown in Fig. 1(b), where one laser pulse is split into two pulses separated by $\tau_0 \pm \Delta\tau$, with $\tau_0 = 3$ ns chosen to be more than three times longer than the lifetime T_1 , so the photons are totally independent. After two excitation pulses, the QD emits two sequential photons that are sent into an all-fibered unbalanced Mach-Zehnder interferometer with a fixed delay τ_0 . We insert in both arms a fibered polarization control setup equivalent to a $\lambda/2$ plate followed by a $\lambda/4$ plate in order to compensate the birefringence induced in the optical fibers. Each output of the interferometer is coupled to a SPAD and for every $\Delta\tau$ we record a histogram of coincidences between the photons arriving on the two detectors, hence extracting the second-order correlation function $g_{\Delta\tau}^{(2)}(\tau)$. Figure 3(a) shows a raw histogram of the detected coincidences for $\Delta\tau = 0$. The five peaks appearing in the central part of the figure correspond to three types of coincidence events. The peak labeled 1 corresponds to the case where the two photons arrive at the same time on the second fibered BS, when the first photon takes the delayed by τ_0 fibered arm and the second photon takes the short arm. Peaks (2,3) and (4,5) correspond to the cases where the two photons arrive on the BS with a delay of $\pm\tau_0$ and $\pm 2\tau_0$, respectively. Other peaks correspond

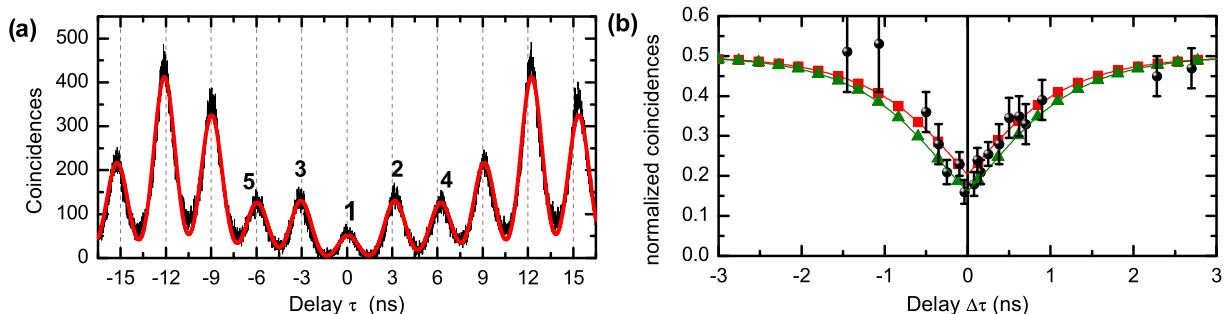


FIG. 3. (Color online) (a) Coincidences histogram (black line) of the two-photon interference experiment for $\Delta\tau = 0$. The red line correspond to a multi-Gaussian fit of the measured histogram. (b) Normalized coincidences showing the Mandel dip. $\Delta\tau$ is the relative delay between the two Mach-Zehnder interferometers on the excitation and detection paths. The red (squares) and green (triangles) lines are theoretical curves of $g_{\Delta\tau}^{(2)}(0)$ for two extreme measured values of T_1 and T_2 (see text).

to coincidences of two photons generated by pair of pulses at ± 12.2 ns, overlapping partially with the five central peaks of interest. The observed asymmetry in the intensity of the side peaks is due to the nonequal reflection R and transmission T coefficients of the BS. At the QD emission wavelength we have measured $R/T = 1.5$. The data are fitted by a multi-Gaussian function, where the ratio of the different peaks area (except for the central one) is determined by the number of correlation events and the values of R and T . The value of $g_{\Delta\tau}^{(2)}(\tau = 0)$ is obtained by dividing the area of peak 1 by the sum of peaks 2 and 3 areas. This quantity defines the conditional probability, given that two photons arrive on the BS at the same time, that the photons exit in opposite directions [6,13]. At $\Delta\tau = 0$, we expect to find $g_0^{(2)}(0) = 0$ for indistinguishable photons and 0.5 for distinguishable photons. By varying the value of $\Delta\tau$, the spatial matching of the two photons can be changed. The measured values of the different $g_{\Delta\tau}^{(2)}(0)$ are shown in Fig. 3(b). The theoretical dependence of the second-order correlation function on the delay time $\Delta\tau$ is given by the expression [16]

$$g_{\Delta\tau}^{(2)}(0) = \frac{1}{2} \left\{ 1 - \frac{2RT}{1-2RT} \left[\frac{T_2}{2T_1} e^{-2|\Delta\tau|/T_2} + \frac{T_2^*}{2T_1} (e^{-|\Delta\tau|/T_1} - e^{-2|\Delta\tau|/T_2}) \right] \right\}. \quad (1)$$

Here, Eq. (1) differs by a factor of 1/2 compared to Eq. (20) in Ref. [16], because we normalize with respect to all the possible coincidence events. T_2^* is a pure dephasing time defined by $\frac{1}{T_2} = \frac{1}{2T_1} + \frac{1}{T_2^*}$ and related among others to the presence of fluctuating charges. From the measured values of T_2 and T_1 we can deduce that $T_2^* \sim 3$ ns, of the same order of magnitude as T_2 , showing that charge noise can have an impact on the coherence properties. The red (squares) and green (triangles) curves in Fig. 3(b) represent the calculated $g_{\Delta\tau}^{(2)}(0)$ using Eq. (1) and correspond to upper and lower bounds with $T_2/2T_1 = 0.64$ and $T_2/2T_1 = 0.71$, respectively,

from the measured values of T_2 and T_1 . The experimental data agree very well with the calculated curves, except for the longest negative delays where a discrepancy is observed. This is likely due to experimental uncertainties coming from fluctuations of the light-QD coupling during the acquisition process, leading to a decrease of the total counts. The error bars represent the signal-to-noise ratio for each measurement. For long delays, the temporal overlap of the two successive photons is reduced and the limit value of 0.5 is reached. As $\Delta\tau$ goes to zero, the two photons interfere constructively, until perfect time matching for $\Delta\tau = 0$ and for totally indistinguishable photons and perfect 50/50 BS, $g_0^{(2)}(0) = 0$. From Eq. (1), $g_0^{(2)}(0) = \frac{1}{2}(1 - \frac{2RT}{1-2RT} \frac{T_2}{2T_1})$ and gives a direct value of the degree of indistinguishability defined by the ratio $T_2/2T_1$. In the case of the probed dot, we measure $T_2/2T_1 = 0.73 \pm 0.05$, which is also in perfect agreement with the direct measurement of $T_2/2T_1 \sim 0.7$.

In summary, we have reported on the observation of the HOM dip for a neutral QD exciton with a strictly resonant pulsed excitation, without any postselection of the emitted photons. All the photons from the luminescence spectrum are coupled to the fibered setup and no polarization filtering is realized in the HOM interferometer. The resonant excitation preserves the coherence and accelerates the radiative lifetime, enhancing by a factor of 7 the ratio $T_2/2T_1$. Therefore, near-unity indistinguishability of single photons could be reached systematically for every dot once fluctuations in the neighboring charge environment are reduced. Applying an electric field in a suitably designed structure could be a way to eliminate this dephasing mechanism and achieve radiatively limited optical linewidths in a controlled way.

The authors thank M. Bernard for technical support and P. Atkinson for helpful discussions. This research is financially supported by the French Agence Nationale de la Recherche (ANR-11-BS10-010) and the C’Nano Ile-de-France (No. 11017728).

-
- [1] For a recent review, see S. Buckley, K. Rivoire, and J. Vuckovic, *Rep. Prog. Phys.* **75**, 126503 (2012), and references therein.
- [2] A. Imamoglu, D. D. Awschalom, G. Burkard, D. P. DiVincenzo, D. Loss, M. Sherwin, and A. Small, *Phys. Rev. Lett.* **83**, 4204 (1999).
- [3] E. Moreau, I. Robert, J. M. Gérard, I. Abram, L. Manin, and V. Thierry-Mieg, *Appl. Phys. Lett.* **79**, 2865 (2001); A. Badolato, K. Hennessy, M. Atatüre, J. Dreiser, E. Hu, P. M. Petroff, and A. Imamoglu, *Science* **308**, 1158 (2005); D. Englund, A. Majumdar, A. Faraon, M. Toishi, N. Stoltz, P. Petroff, and J. Vuckovic, *Phys. Rev. Lett.* **104**, 073904 (2010); J. Claudon, J. Bleuse, N. S. Malik, M. Bazin, P. Jaffrennou, N. Gregersen, C. Sauvan, P. Lalanne, and J.-M. Gérard, *Nat. Photonics* **4**, 174 (2010); A. Dousse, L. Lanco, J. J. Suffczyński, E. Semenova, A. Miard, A. Lemaître, I. Sagnes, C. Roblin, J. Bloch, and P. Senellart, *Phys. Rev. Lett.* **101**, 267404 (2008).
- [4] E. Knill, R. Lafamme, and G. J. Milburn, *Nature (London)* **409**, 46 (2001); A. Kiraz, M. Atatüre, and A. Imamoglu, *Phys. Rev. A* **69**, 032305 (2004).
- [5] C. K. Hong, Z. Y. Ou, and L. Mandel, *Phys. Rev. Lett.* **59**, 2044 (1987).
- [6] S. Varoutsis, S. Laurent, P. Kramper, A. Lemaître, I. Sagnes, I. Robert-Philip, and I. Abram, *Phys. Rev. B* **72**, 041303(R) (2005).
- [7] S. Weiler, A. Ulhaq, S. M. Ulrich, S. Reitzenstein, A. Löffler, A. Forchel and P. Michler, *Phys. Status Solidi B* **248**, 867 (2011).
- [8] R. B. Patel, A. J. Bennett, K. Cooper, P. Atkinson, C. A. Nicoll, D. A. Ritchie, and A. J. Shields, *Phys. Rev. Lett.* **100**, 207405 (2008).
- [9] Q. Q. Wang, A. Muller, P. Bianucci, E. Rossi, Q. K. Xue, T. Takagahara, C. Piermarocchi, A. H. MacDonald, and C. K. Shih, *Phys. Rev. B* **72**, 035306 (2005); P. Borri, W. Langbein, S. Schneider, U. Woggon, R. L. Sellin, D. Ouyang, and D. Bimberg, *ibid.* **66**, 081306(R) (2002); A. J. Ramsay, A. Venu Gopal, E. M. Gauger, A. Nazir, B. W. Lovett, A. M. Fox, and M. S. Skolnick, *Phys. Rev. Lett.* **104**, 017402 (2010); A. J. Ramsay, T. M. Godden, S. J. Boyle, E. M. Gauger, A. Nazir, B. W. Lovett, A. M. Fox, and M. S. Skolnick, *ibid.* **105**, 177402 (2010).

- [10] A. Muller, E. B. Flagg, P. Bianucci, X. Y. Wang, D. G. Deppe, W. Ma, J. Zhang, G. J. Salamo, M. Xiao, and C. K. Shih, *Phys. Rev. Lett.* **99**, 187402 (2007); R. Melet, V. Voliotis, A. Enderlin, D. Roditchev, X. L. Wang, T. Guillet, and R. Grousson, *Phys. Rev. B* **78**, 073301 (2008); H. S. Nguyen, G. Sallen, C. Voisin, Ph. Roussignol, C. Diederichs, and G. Cassaboïs, *Appl. Phys. Lett.* **99**, 261904 (2011); C. Matthiesen, A. N. Vamivakas, and M. Atature, *Phys. Rev. Lett.* **108**, 093602 (2012); S. Ates, S. M. Ulrich, S. Reitzenstein, A. Löffler, A. Forchel, and P. Michler, *ibid.* **103**, 167402 (2009).
- [11] P. Domokos, P. Horak, and H. Ritsch, *Phys. Rev. A* **65**, 033832 (2002).
- [12] L. Monniello, C. Tonin, R. Hostein, A. Lemaitre, A. Martinez, V. Voliotis, and R. Grousson, *Phys. Rev. Lett.* **111**, 026403 (2013).
- [13] C. Santori, D. Fattal, J. Vuckovic, G. Salomon, and Y. Yamamoto, *Nature (London)* **419**, 594 (2002).
- [14] Y.-M. He, Y. He, Y.-J. Wei, D. Wu, M. Atatüre, C. Schneider, S. Höfling, M. Kamp, C.-Y. Lu, and J.-W. Pan, *Nat. Nanotechnol.* **8**, 213 (2013).
- [15] E. B. Flagg, A. Muller, S. V. Polyakov, A. Ling, A. Migdall, and G. S. Salomon, *Phys. Rev. Lett.* **104**, 137401 (2010); R. Patel, A. Bennett, I. Farrer, C. Nicoll, A. Ritchie, and A. Shields, *Nat. Photonics* **4**, 632 (2010); T. Kuroda *et al.*, *Phys. Rev. B* **88**, 041306(R) (2013); P. Gold, A. Thoma, S. Maier, S. Reitzenstein, C. Schneider, S. Höfling, and M. Kamp, *ibid.* **89**, 035313 (2014).
- [16] J. Bylander, I. Robert-Philip, and I. Abram, *Eur. Phys. J. D* **22**, 295 (2003).
- [17] C. Tonin, R. Hostein, V. Voliotis, R. Grousson, A. Lemaitre, and A. Martinez, *Phys. Rev. B* **85**, 155303 (2012).
- [18] H. S. Nguyen, G. Sallen, M. Abbarchi, R. Ferreira, C. Voisin, Ph. Roussignol, G. Cassaboïs, and C. Diederichs, *Phys. Rev. B* **87**, 115305 (2013); H. S. Nguyen, G. Sallen, C. Voisin, Ph. Roussignol, C. Diederichs, and G. Cassaboïs, *Phys. Rev. Lett.* **108**, 057401 (2012).
- [19] D. Elvira, R. Hostein, B. Fain, L. Monniello, A. Michon, G. Beaudoin, R. Braive, I. Robert-Philip, I. Abram, I. Sagnes, and A. Beveratos, *Phys. Rev. B* **84**, 195302 (2011).
- [20] C. Cohen Tannoudji, J. Dupont-Roc, and G. Grynberg, *Atom-Photon Interactions: Basic Processes and Applications* (Wiley, New York, 1992).
- [21] E. M. Purcell, H. C. Torrey, and R. V. Pound, *Phys. Rev.* **69**, 37 (1946).
- [22] J. Houel, A. V. Kuhlmann, L. Greuter, F. Xue, M. Poggio, B. D. Gerardot, P. A. Dalgarno, A. Badolato, P. M. Petroff, A. Ludwig, D. Reuter, A. D. Wieck, and R. J. Warburton, *Phys. Rev. Lett.* **108**, 107401 (2012).
- [23] A. Berthelot, I. Favero, G. Cassaboïs, C. Voisin, C. Delalande, Ph. Roussignol, R. Ferreira, and J. M. Gerard, *Nat. Phys.* **2**, 759 (2006).
- [24] R. Loudon, *Quantum Theory of Light*, 3rd ed. (Oxford University Press, New York, 2000).